

Analytical approach to the Davydov-Scott theory with on-site potential

Yaroslav Zolotaryuk^{*,†} and J. Chris Eilbeck^{*}

^{*}*Department of Mathematics, Heriot-Watt University, Edinburgh EH14 4 AS, UK*

[†]*Max-Planck-Institut für Physik Komplexer Systeme, Nöthnitzer Str. 38, 01187 Dresden, Germany*
(August 10, 2000)

We propose an analytical approach to study the one-dimensional acoustic polaron model that includes an on-site external potential applied to each chain molecule. The key to the approach is an exact discrete solution for the chain deformation field given in terms of a (quasi)particle wavefunction. For this purpose we introduce a whole variety of polynomial series which resemble the Chebyshev polynomials. We call these series the hyperbolic Chebyshev polynomials. Using next a properly chosen discrete trial function for the wavefunction envelope, we obtain simple expressions for the variational energy of the system. Contrary to an isolated molecular chain, the polaron state (Davydov soliton) is shown to exist only for appropriate system parameters while the delocalized (exciton) state can always exist. As a result, the following three regimes can be specified for the chain with an on-site potential: (i) the polaron is a ground state and the exciton is a metastable state, (ii) the polaron is a metastable state and the exciton is a (delocalized) ground state, and (iii) the polaron state does not exist and only the exciton exists, being a ground state. Two characteristic dimensionless parameters are found in terms of which a criterion of existence of (stable and metastable) polaron states and their non-existence is formulated. Finally, pinning barrier for the Davydov soliton is found to vanish in a particular case of system parameters, resulting in a transparent regime of uniform propagation of the soliton with very small size.

I. INTRODUCTION

There has been renewed interest in the Davydov soliton and polarons in molecular chains [1,2] demonstrated by recent publications [3–15], which have called into question different aspects of polaron dynamics and self-trapping. Historically, one-dimensional polaron models received a major impetus from the work of Davydov and Kislukha [16], who used the exciton formalism to describe the steady-state propagation of a self-localized intramolecular excitation (generally, a quantum particle) along a molecular (polypeptide) chain. This transfer process, often referred to as the Davydov-Scott self-trapping mechanism of energy transfer in protein, involves high-frequency intramolecular motions (considered by Takeno [17] as classical oscillators) which are coupled to low-frequency acoustic (as in the original Davydov model [1–3,7,8,16,18]) or optical (as in the Holstein model [4,6,9–13,19–21]) phonon motions.

The purpose of the present paper is to investigate the problem of existence of self-localized (polaron) states in a molecular chain interacting with its environment, contrary to the original acoustic Davydov model in which the chain of coupled massive molecules is considered as an isolated object. Thus, each hydrogen-bonded molecular chain in the α -helix protein or in crystalline acetanilide [20,21] is tightly coupled to a three-dimensional complex skeleton and therefore each molecule of the chain has an equilibrium position given externally. The simplest way to describe the interaction of the molecular chain with such an atomic or molecular periodic environment is to introduce in the acoustic Davydov Hamiltonian a sequence of harmonic on-site potentials and to place each chain molecule in this potential, allowing it to vibrate with low frequency around the potential bottom [15,22,23]. Thus, our generalized polaron Hamiltonian consists of three parts:

$$\hat{H} = \hat{H}_{\text{qp}} + \hat{H}_{\text{ph}} + \hat{H}_{\text{qp-ph}} \quad (1)$$

where \hat{H}_{qp} describes a single free quantum particle or quasiparticle (an exciton or an extra electron) in the chain, \hat{H}_{ph} is the phonon Hamiltonian, and $\hat{H}_{\text{qp-ph}}$ describes the interaction of the quantum (quasi)particle with acoustic phonons of the chain.

The first term in the r.h.s. of Eq. (1) is the usual tight binding Hamiltonian for a quantum (quasi)particle:

$$\hat{H}_{\text{qp}} = \sum_n \left[\mathcal{E}_0 a_n^\dagger a_n - J(a_n^\dagger a_{n+1} + a_{n+1}^\dagger a_n) \right] \quad (2)$$

where \mathcal{E}_0 is the (quasi)particle energy in the undistorted chain, J the hopping amplitude (e.g., the dipole-dipole interaction strength between intramolecular vibrations, when the chain is undistorted), and a_n^\dagger (a_n) are the Bose or Fermi creation (annihilation) operators of the (quasi)particle associated with the n th molecule of the chain.

The second part of Eq. (1) describes the phonon displacement field \hat{Q}_n interacting (in the harmonic approximation) with a periodic substrate potential, so that each chain molecule is assumed to be influenced by the local harmonic potential with a force constant κ_0 :

$$\hat{H}_{\text{ph}} = \sum_n \left[\frac{\hat{P}_n^2}{2M} + \frac{K}{2}(\hat{Q}_{n+1} - \hat{Q}_n)^2 + \frac{\kappa_0}{2}\hat{Q}_n^2 \right]. \quad (3)$$

Here M is the molecular mass, K is the force constant of the interaction between molecules, and the lattice field operators \hat{P}_n and \hat{Q}_n are the momentum and displacement from the equilibrium position of the n th chain molecule.

The third part of the Hamiltonian \hat{H} describes the (quasi)particle-phonon interaction which consists of two portions [18]. One of these appears under the assumption that (quasi)particle band energy depends linearly on the distance between the nearest-neighbour molecules as $\mathcal{E}_n = \mathcal{E}_0 + \chi_1(Q_{n+1} - Q_{n-1})$, whereas the appearance of the other interaction term is associated with the linear dependence of the amplitude of hopping between the n th and $(n+1)$ th molecules: $J_{n,n+1} = J - \chi_2(Q_{n+1} - Q_n)$, meaning that the hopping amplitude decreases with increase of the distance between the adjacent molecules. Thus, the Hamiltonian that describes such a combined (quasi)particle-interaction and was also introduced in earlier studies [18,24] reads

$$\hat{H}_{\text{qp-ph}} = \chi_1 \sum_n a_n^\dagger a_n (\hat{Q}_{n+1} - \hat{Q}_{n-1}) + \chi_2 \sum_n (a_n^\dagger a_{n+1} + a_{n+1}^\dagger a_n) (\hat{Q}_{n+1} - \hat{Q}_n). \quad (4)$$

Using the adiabatic Davydov ansatz [1,2] with the corresponding techniques [25], one finds that the Hamiltonian (1)-(4) results in the following system of two coupled classical equations of motion:

$$i\hbar\dot{\psi}_n = \mathcal{E}_0\psi_n - J(\psi_{n-1} + \psi_{n+1}) + \chi_1(Q_{n+1} - Q_{n-1})\psi_n + \chi_2[(Q_n - Q_{n-1})\psi_{n-1} + (Q_{n+1} - Q_n)\psi_{n+1}], \quad (5)$$

$$\ddot{Q}_n = K(Q_{n+1} - 2Q_n + Q_{n-1}) - \kappa_0 Q_n + \chi_1(|\psi_{n+1}|^2 - |\psi_{n-1}|^2) + 2\chi_2\text{Re}[\psi_n^*(\psi_{n+1} - \psi_{n-1})], \quad (6)$$

where $\psi_n(t)$ is the discrete complex-valued wavefunction of the (quasi)particle and $Q_n(t)$ the classical lattice field of the molecule's displacements from their equilibrium positions, $n = 0, \pm 1, \dots$. These equations are complemented by the normalization condition $\sum_n |\psi_n(t)|^2 = 1$.

In the particular case when the phonon term with the on-site oscillators is absent ($\kappa_0 = 0$), Eqs. (5) and (6) reduce to the usual Davydov model [1,2]. In this case, each of the (quasi)particle-phonon coupling constants χ_1 or χ_2 results in the existence of self-localized states for all values of the system parameters. Moreover, Eqs. (5) and (6) are easily solved in the continuum limit and the self-trapping occurs with the additive coupling constant $\chi = \chi_1 + \chi_2$. Therefore the interaction term with χ_2 was rarely considered in literature. However, the situation in the anticontinuum limit appears to be more sophisticated because the physical origin of the constants χ_1 and χ_2 is different: the interaction with χ_1 is a result of lowering the on-site energy \mathcal{E}_n under a chain compression, whereas the second (χ_2) interaction originates from increase of the hopping amplitude $J_{n,n+1}$ with this compression. Therefore it is not clear what happens to a small (narrow) Davydov soliton when both these interactions are present in the theory. The present paper also aims to investigate how the interplay between the constants χ_1 and χ_2 results in mobility of the Davydov soliton.

On the other hand, the Hamiltonian (1)-(4) may also be referred to as the Holstein model [19] with a positive (because $K > 0$) dispersion and a nonlocal electron-phonon coupling (with the two constants $\chi_1 \geq 0$ and $\chi_2 \geq 0$). We consider the following arguments. In the limiting case $K \rightarrow 0$, when the coupling between the on-site oscillators is absent (it occurs only via the nonlocal electron-phonon coupling), it is not known whether polaron solutions exist. Indeed, in the continuum limit (when the site n is substituted by the spatial variable x), for the standing continuum envelope $\varphi(x)$ of the wavefunction $\psi_n(t)$ one can derive from (5) and (6) the nonlinear Schrödinger equation with the nonlinearity $(\varphi^2)''\varphi$ (where the prime denotes the differentiation over x) which can easily be integrated and analyzed using phase portrait techniques. As a result, this equation appears not to support solutions of the standard (bell-shaped) type which would correspond to self-localized states.

However, if we consider the discrete version of this model, using a variational approach (used in the present paper) to find the envelope φ_n in the form of a discrete trial function with exponential spatial decay, we find that, contrary to the continuum limit, the total energy of the system attains a minimum, but only if the constant $\chi_1^2/J\kappa_0$ exceeds a certain critical value. This means that there exists some critical value for the eigenfrequency of the on-site oscillators, above which the self-trapping effect disappears. The phonon dispersion should effectively soften this frequency, so that the critical value will increase. This is why for the Davydov model with an on-site potential, the existence of self-localized states in some cases was numerically observed, but in other cases only delocalised states were obtained

[22]. All these arguments demonstrate that the problem of the existence of self-localized states in the polaron model given by the Hamiltonian (1)-(4) is far from being fully understood.

The results in the present paper are obtained in two steps. First, we develop analytical techniques of summation of the whole variety of series using an algebra that is similar to that of the Chebyshev polynomials. This allows us to obtain all equations expressed only in terms of the envelope φ_n . Second, having in the theory only one lattice field φ_n , we are able to apply a simple variational approach using only *one* variational parameter. In this way, it is proved that final equations can be analyzed analytically. Particularly, a criterion for the existence of self-localised (both stable and metastable) states is obtained.

This paper is organized as follows. In the next section, we present the reduced equations of motion which are basic equations to be studied throughout this paper. In Sec. III, using the Chebyshev-like polynomials, we develop a procedure that gives an analytical solution for the lattice displacement field as a function of the wavefunction envelope. In the next section, we apply a discrete variational approach to find this envelope by minimization. A criterion given as an implicit function of two dimensionless characteristic parameters is derived in Sec. V. The binding energy of the localized (quasi)particle is discussed in Sec. VI. This section also confirms a high accuracy of our variational approach. In Sec. VII, we estimate the Peierls-Nabarro barrier for the self-localized states and find the particular case when polarons are depinned. Section VIII contains our conclusions. Finally, some results of analytical calculations are presented in Appendices A and B.

II. REDUCED EQUATIONS TO BE STUDIED

For the dimensionless description we introduce scaled time $\tau = v_0 t/l$, where l is the lattice spacing and $v_0 = \sqrt{K/M} l$ the sound velocity in the lattice subsystem. In terms of the space and time scaling parameters, both the (quasi)particle wavefunction $\psi_n(t)$ and the displacement field $Q_n(t)$ can be rewritten as $\phi_n(\tau) = \exp[i(E_0 - 2J)t/\hbar] \psi_n(t)$ and $u_n(\tau) = Q_n(t)/l$. Next, we use the representation of the wavefunction $\phi_n(\tau)$ in the form of a modulated plane wave:

$$\phi_n(\tau) = \varphi_n(\tau) \exp\{i[nk - \sigma(\varepsilon_0 + \varepsilon)\tau]\} \quad (7)$$

where the characteristic parameter $\sigma = Jl/\hbar v_0$ measures the ratio of amplitudes for transfers from site to site in the (quasi)particle and phonon subsystems. Thus, for α -helix protein, the values $J = 7.8 \text{ cm}^{-1}$ and $l = 4.5 \text{ \AA}$ are known [18], so that for velocities $v_0 \sim 10^3 \text{ m/s}$ one obtains $\sigma \sim 1$. The dimensionless energy $\varepsilon_0 = 2(1 - \cos k)$ describes the linear band spectrum of the linearized equation (5) and ε is the binding energy of the (quasi)particle to the chain. Using the representation (7) in (5) and (6) and equating the real and imaginary parts of (5), we find the following three discrete equations:

$$= \varepsilon \varphi_n = -\cos k (\varphi_{n+1} - 2\varphi_n + \varphi_{n-1}) + (\alpha/2) \{ (1 - \eta)(u_{n+1} - u_{n-1})\varphi_n + \eta \cos k [(u_n - u_{n-1})\varphi_{n-1} + (u_{n+1} - u_n)\varphi_{n+1}] \}, \quad (8)$$

$$\frac{d\varphi_n}{d\tau} = \sin k \{ \sigma(\varphi_{n-1} - \varphi_{n+1}) + (\alpha\eta/2)[(u_{n+1} - u_n)\varphi_{n+1} - (u_n - u_{n-1})\varphi_{n-1}] \}, \quad (9)$$

$$\frac{d^2 u_n}{d\tau^2} = -(u_{n+1} - 2u_n + u_{n-1}) - \omega_0^2 u_n + \beta [(1 - \eta) (\varphi_{n+1}^2 - \varphi_{n-1}^2) / 2 + \eta \cos k \varphi_n (\varphi_{n+1} - \varphi_{n-1})]. \quad (10)$$

In these equations, the coupling constants χ_1 and χ_2 are redefined to the dimensionless quantities α and β according to the relations $\alpha = 2l(\chi_1 + \chi_2)/J$ and $\beta = 2l(\chi_1 + \chi_2)/Mv_0^2$ [23]. We have also incorporated the partition parameter $\eta = \chi_2/(\chi_1 + \chi_2)$, $0 \leq \eta \leq 1$, so that $\eta = 0$ if $\chi_2 = 0$ and $\eta = 1$ if $\chi_1 = 0$ [24]. The dimensionless frequency $\omega_0 = \sqrt{\kappa_0/K}$ measures the relative strength of the intermolecular and on-site interactions. Note that the former interactions effectively reduce the eigenfrequency of the on-site oscillators. Finally, the envelope $\varphi_n(\tau)$ satisfies the normalization condition

$$\sum_n \varphi_n^2 = 1. \quad (11)$$

The reduced equations (8)-(11) are the key object to be studied in the present paper. As regard the spectral parameter ε in (8), it can be expressed in terms of the lattice fields φ_n and u_n as follows. Multiplying both the sides of (8) by φ_n and summing them over n , and then using the normalization condition (11), we find

$$\begin{aligned} \varepsilon = \text{cos}k \sum_n (\varphi_{n+1} - \varphi_n)^2 + \frac{1}{2} \alpha \sum_n (1 - \eta)(u_{n+1} - u_{n-1})\varphi_n \\ + \frac{1}{2} \alpha \eta \text{cos}k [(u_n - u_{n-1})\varphi_{n-1} + (u_{n+1} - u_n)\varphi_{n+1}]. \end{aligned} \quad (12)$$

In this paper we are interested only in travelling wave (TW) solutions of (8)–(11). For this class of solutions one can write $\varphi_n(\tau) = \varphi(n - s\tau)$ and $u_n(\tau) = u(n - s\tau)$ where $s = v/v_0$ is the dimensionless propagation velocity. Then in the continuum limit, (9) is transformed to the relation between the wavenumber k and the velocity of wave propagation s :

$$s = 2\sigma \text{sin}k. \quad (13)$$

Note that in the particular case of standing solutions ($s = 0$), Eq. (9) simply vanishes ($k = 0$). As for Eq. (10), in the continuum limit (again for TW solutions) one can approximately substitute the time derivative by the discrete time derivative: $d^2u_n/d\tau^2 \simeq s^2(u_{n+1} - 2u_n + u_{n-1})$. Then this equation can be rewritten concisely as

$$u_{n+1} - 2\zeta u_n + u_{n-1} = R_n \quad (14)$$

with the source term

$$R_n = G(1 - \eta) (\varphi_{n-1}^2 - \varphi_{n+1}^2) + 2G\eta \text{cos}k \varphi_n (\varphi_{n-1} - \varphi_{n+1}). \quad (15)$$

Here the constants ζ and G are defined by $\zeta = 1 + \omega_0^2/2(1 - s^2)$ and $G = \beta/2(1 - s^2)$. Therefore (14) is appropriate for moving ($s > 0$) solutions if they are sufficiently smooth from site to site, but it also appears as an exact *discrete* equation for standing ($k = 0$ and $s = 0$) solutions.

As mentioned in the previous section, in the limiting case when the on-site potential disappears ($\omega_0 \rightarrow 0$ or $\zeta \rightarrow 1$), the system of equations (8) and (14) is reduced to the usual acoustic polaron model [1,2]. In this particular case, the difference $u_{n+1} - u_n$ can easily be found from (14) and (15) as a function of φ_n and φ_{n+1} . Inserting this function into (8), we obtain a stationary discrete nonlinear Schrödinger (DNLS) equation with cubic nonlinearity, the normalized solution of which in the continuum limit is well known: $\varphi_n(\tau) = \sqrt{\lambda/2} \text{sech}[\lambda(n - s\tau)]$ and $\varepsilon = -\lambda^2 \text{cos}k$ with the reduced coupling constant

$$\lambda = \alpha\beta (1 - \eta + \eta \text{cos}k)^2 / 4(1 - s^2) \text{cos}k. \quad (16)$$

For instance, in the case of α -helix protein, the mass of a peptide group is $M = 114 m_p$, where m_p is the proton mass and the coupling constant was estimated as $\chi_1 = 3.4 \times 10^{-11}$ N. Therefore, the constant λ at $k = 0$ is of order 10. Note also that for $k = 0$, the constant λ does not depend on the partition parameter η because both the constants χ_1 and χ_2 are present in the theory additively. As can be seen from this solution, the constant λ is a characteristic parameter of the theory, since it determines the soliton size and the energy level ε .

III. DECOUPLING PROCEDURE AND HYPERBOLIC CHEBYSHEV POLYNOMIALS

In a general case when $\zeta > 1$, we cannot express so easily the difference $u_{n+1} - u_n$ through the envelope φ_n as in the limiting case $\zeta \rightarrow 1$. But this step is necessary in order to get a nonlinear Schrödinger equation given in terms of only φ_n . In this section, using the explicit representation of Chebyshev-like polynomials, we develop a procedure which allows us to solve this problem. This is the most important point of our findings. In this way we are able to decouple the lattice fields φ_n and u_n and we call this scheme a decoupling procedure.

Let us consider solutions of the two types of symmetry: the centre of the φ_n profile is assumed to be localized at a lattice site (we call it a site-centred or *S* state) and the φ_n profile is centred in the middle of adjacent lattice sites (call it a bond-centred or *B* state). Next, let us suppose the φ_n profile to be centred at the site with $n = 0$. Then one can write $\varphi_{-n} = \varphi_n$ ($n = 0, \pm 1, \dots$). In the other case, assuming that the φ_n profile is centred in the middle between the sites with $n = 0$ and $n = 1$, we have $\varphi_{-n} = \varphi_{n+1}$ ($n = 0, \pm 1, \dots$). Using these symmetry definitions in (15), we find that $R_{-n} = -R_n$ and $R_{-n} = -R_{n+1}$, $n = 0, \pm 1, \dots$, for the site- and bond-centred profiles, respectively. Using the last relations, one finds from (14) the symmetry properties of the displacement field u_n . Thus, the *S* and *B* symmetry properties can be summarized as follows

$$\varphi_{-n} = \varphi_n, \quad u_{-n} = -u_n, \quad R_{-n} = -R_n \quad (17)$$

for *S* symmetry and

$$\varphi_{-n} = \varphi_{n+1}, \quad u_{-n} = -u_{n+1}, \quad R_{-n} = -R_{n+1} \quad (18)$$

for *B* symmetry, where $n = 0, \pm 1, \dots$. Below we treat self-localized states of both symmetries separately.

A. Site-centred self-localized states

In the case of solutions centred at the site with $n = 0$, we have the identities $R_0 = 0$ and $u_0 = 0$, which immediately follow from the symmetry relations (17). Next, by induction, one can prove that the solution of the linear difference equation (14) can be represented in the form

$$u_n = K_{n-1}^{[2\zeta]} u_1 + \sum_{j=1}^{n-1} K_{n-1-j}^{[2\zeta]} R_j, \quad n = 2, 3, \dots, \quad (19)$$

where $K_n^{[2\zeta]} = K_n^{[2\zeta]}(\zeta)$ is the Green's function defined by the recurrence formula

$$K_{n+2}^{[f(\zeta)]}(\zeta) = 2\zeta K_{n+1}^{[f(\zeta)]}(\zeta) - K_n^{[f(\zeta)]}(\zeta), \quad K_0^{[f(\zeta)]}(\zeta) = 1, \quad K_1^{[f(\zeta)]}(\zeta) = f(\zeta), \quad (20)$$

with a generating function $f(\zeta)$ indicated in the square brackets superscript. It is important that in the particular case when the generating function is $f(\zeta) = \zeta$, $1 \leq \zeta < \infty$, the functions $K_n^{[f(\zeta)]}$ can be calculated explicitly:

$$K_n^{[\zeta]}(\zeta) \equiv T_n(\zeta) = \cosh(n \operatorname{Arcosh} \zeta) = (b^n + b^{-n})/2, \quad b = \zeta + \sqrt{\zeta^2 - 1}, \quad (21)$$

for all integers $n = 0, 1, \dots$. Since the algebra of these is ‘‘hyperbolic’’, contrary to the usual Chebyshev polynomials defined on the interval $0 \leq \zeta \leq 1$, we call the set of functions (21) the *hyperbolic* Chebyshev polynomials.

The next important step is that the $K_n^{[2\zeta]}$ polynomials, including also those with other generating functions $f(\zeta)$, can be expressed explicitly in terms of the polynomials $T_n(\zeta)$. Indeed, by induction, one can establish the identity

$$K_n^{[2\zeta]} - K_{n-2}^{[2\zeta]} = 2T_n, \quad n = 2, 3, \dots \quad (22)$$

Using this identity, we find separately for even and odd subscripts the relations that allow us to write the functions $K_n^{[2\zeta]}$ through the polynomials T_n :

$$K_{2m}^{[2\zeta]} = 1 + 2 \sum_{j=1}^m T_{2j}, \quad m = 1, 2, \dots; \quad K_{2m+1}^{[2\zeta]} = 2 \sum_{j=0}^m T_{2j+1}, \quad m = 0, 1, \dots \quad (23)$$

Finally, using the representation (23) and the explicit formula (21), one finds the explicit expression for the polynomials $K_n^{[2\zeta]}$:

$$K_n^{[2\zeta]} = \frac{b^{n+1} - b^{-n-1}}{b - b^{-1}}, \quad n = 0, 1, \dots \quad (24)$$

Now we need to calculate the displacement u_1 in (19). To this end, we use a boundary condition at the right end of the chain. Particularly, using the zero boundary condition ($\lim_{n \rightarrow \infty} u_n = 0$), we find from (19):

$$u_1 = - \lim_{n \rightarrow \infty} \sum_{j=1}^{n-1} \left[K_{n-1-j}^{[2\zeta]} / K_{n-1}^{[2\zeta]} \right] R_j = - \lim_{n \rightarrow \infty} \sum_{j=1}^{n-1} \frac{b^{n-j} - b^{-n+j}}{b^n - b^{-n}} R_j = - \sum_{j=1}^{\infty} b^{-j} R_j. \quad (25)$$

Thus, (19), (24), and (25) determine the displacement field u_n , $n = 1, 2, \dots$, as a function of the envelope φ_n for each $\zeta > 1$. Calculating next the relative displacements $u_{n+1} - u_n$ in terms of φ_n and substituting the resulting expressions into (8), we obtain a stationary discrete nonlinear Schrödinger (DNLS) equation. In the two particular cases $\eta = 0$ ($\chi_2 = 0$) and $\eta = 1$ ($\chi_1 = 0$), this equation is derived in Appendix A [see (A4) and (A9)].

B. Bond-centred self-localized states

In the case of solutions centred in the middle between the sites with $n = 0$ and $n = 1$, the symmetry properties are determined by Eqs. (18). Using the equation $u_0 = -u_1$, by induction, one can prove that the solution of the linear difference equation (14) is represented in the form

$$u_n = K_{n-1}^{[2\zeta+1]} u_1 + \sum_{j=1}^{n-1} K_{n-1-j}^{[2\zeta]} R_j, \quad n = 2, 3, \dots, \quad (26)$$

where the polynomials $K_n^{[2\zeta+1]}$ can also be expressed in terms of the hyperbolic Chebyshev polynomials T_n . Similarly, by induction, one can establish the identity

$$K_n^{[2\zeta+1]}(\zeta) = K_{n-1}^{[2\zeta]}(\zeta) + K_n^{[2\zeta]}(\zeta), \quad n = 1, 2, \dots \quad (27)$$

Using this equation and the representation (24), we find the explicit expression for the polynomials $K_n^{[2\zeta+1]}$:

$$K_n^{[2\zeta+1]} = \frac{b^{n+1} - b^{-n}}{b - 1}, \quad n = 0, 1, \dots \quad (28)$$

In the same way as for the S profiles, the displacement u_1 can be calculated, using the zero boundary condition at the right end of the chain. As a result, from Eq. (26) we find

$$u_1 = - \lim_{n \rightarrow \infty} \sum_{j=1}^{n-1} \left[K_{n-1-j}^{[2\zeta]} / K_{n-1}^{[2\zeta+1]} \right] R_j = - \lim_{n \rightarrow \infty} \sum_{j=1}^{n-1} \frac{b^{n-j} - b^{-n+j}}{(b+1)(b^{n-1} - b^{-n})} R_j = - \frac{1}{1+b^{-1}} \sum_{j=1}^{\infty} b^{-j} R_j. \quad (29)$$

The corresponding DNLS equations are given by (A14) and (A18).

IV. CALCULATION OF SELF-LOCALIZED STATES

When $\omega_0 \neq 0$ ($b > 1$), each of the stationary DNLS equations (A4), (A9), (A14), or (A18) cannot be solved analytically, because even in the continuum limit it becomes an integro-differential equation. Therefore an appropriate variational method should be applied. From this point of view, the exact representations for the lattice displacement field u_n given by the series (A2), (A7), (A12), and (A16) with the corresponding coefficients A_{jn} , B_{jn} , C_{jn} , and D_{jn} (see (A3), (A8), (13), and (A17)) appear to be very useful because they allow us to reduce significantly the number of variational parameters. We use a discrete trial function with only *one* variational parameter describing the size of self-localization. As a result, the polaron profiles and energy are found in a simple form.

First, we notice that the basic equations (8) and (14) can be represented as a minimum condition for the discrete energy functional $E(\{\varphi_n\}, \{u_n\})$, written through the reduced Lagrangian function L :

$$E = -L = \text{cos}k \sum_n [(\varphi_{n+1} - \varphi_n)^2 + (\alpha/2G \text{cos}k) u_n (R_n + \zeta u_n - u_{n+1})], \quad \zeta = (b + b^{-1})/2, \quad (30)$$

where the constant term with ε has been omitted. This functional can also be obtained in the standard manner (as for the equations of motion (5) and (6)) from the Hamiltonian (1)-(4), using the same assumptions and notation that led to (8) and (14). Inserting the representation for u_n given by (A2), (A7), (A12), and (A16) into (30), we get the functional of *one* lattice field, i.e., $E(\{\varphi_n\})$. Therefore a properly chosen discrete trial function with only one variational parameter can be used and its optimal value can be calculated analytically by minimization of the variational energy (30). Below we will apply this variational approach separately to the S and B polaron states.

A. Site-centred self-localized states

Thus, for the S polaron states, the trial function that describes the normalized (see (11)) envelope profile φ_n can be chosen in the form

$$\varphi_n = \sqrt{\frac{1-q^2}{1+q^2}} q^n, \quad n = 0, \pm 1, \dots \quad (31)$$

Then, according to (A2) and (A7), we find by straightforward calculation that the displacement field u_n is given by $u_0 = 0$ and

$$u_n = \frac{b(1-q^2)^2 (q^{2n} - b^{-n})}{(1-bq^2)(b-q^2)} G \quad (32)$$

if $\eta = 0$ and

$$u_n = \frac{2bq(1-q^2)^2(q^{2n}-b^{-n})}{(1+q^2)(1-bq^2)(b-q^2)} G \cos k \quad (33)$$

if $\eta = 1$, where $n = 1, 2, \dots$. Inserting next the expressions (31)-(33) into the functional (30) and using the symmetry properties of the lattice fields φ_n and u_n (see (17)) as well as the definitions (15), (A5), and (A10), by direct but lengthy calculations we obtain

$$\frac{E_{S\nu}(b, \lambda_\nu; q)}{\cos k} = 2 \frac{(1-q)^2}{1+q^2} - \lambda_\nu \frac{(1-q^2)^3}{(b-q^2)^2} P_{S\nu}(b; q), \quad \nu = 0, 1, \quad (34)$$

where the subscript $\nu = 0$ ($\nu = 1$) corresponds to the case $\eta = 0$ ($\eta = 1$) and the functions $P_{S\nu}(b; q)$ are presented in Appendix B (see (B1)). Note that both the functions $P_{S\nu}$ have small variation in the interval $0 \leq q \leq 1$ and tend to $b/2$ when $q \rightarrow 1$.

B. Bond-centred self-localized states

For the B polaron states the trial function for the envelope φ_n can be chosen in the form

$$\varphi_n = \sqrt{\frac{1-q^2}{2}} q^{n-1}, \quad n = 1, 2, \dots \quad (35)$$

Similarly, according to (A12), (A13), (A16), and (A17), we find

$$u_n = \frac{b(1-q^2)^2 [(1+q^{-2})q^{2n} - (b+1)b^{-n}]}{2(1-bq^2)(b-q^2)} G, \quad (36)$$

if $\eta = 0$ and

$$u_n = \frac{b(1-q^2)^2}{(1-bq^2)(b-q^2)} \left[q^{2n-1} - \frac{q(1-bq^2) + b(bq + q + 1 + q^2)}{(b+1)(1+q)} b^{-n} \right] G \cos k \quad (37)$$

if $\eta = 1$, where $n = 1, 2, \dots$. Next, using in the same manner as above the symmetry properties of the lattice fields φ_n and u_n given by Eqs. (18) as well as the expressions (35)-(37), we find that the energy functional (30) is transformed to

$$\frac{E_{B\nu}(b, \lambda_\nu; q)}{\cos k} = (1-q)^2 - \lambda_\nu \frac{(1-q^2)^3}{(b-q^2)^2} P_{B\nu}(b; q), \quad \nu = 0, 1, \quad (38)$$

where the explicit form of the functions $P_{B\nu}$ is also presented in Appendix B (see (B1)). As above, these functions also tend to $b/2$ if $q \rightarrow 1$.

C. Energy surfaces and delocalized states

The four variational functions $E_{S\nu}(b, \lambda_\nu; q)$ and $E_{B\nu}(b, \lambda_\nu; q)$, $\nu = 0, 1$, given by (34) and (38) is the basic result of the analytical approach developed in this paper. The two-dimensional plots of one of these functions, namely $\Phi_0(q) \equiv E_{S0}(b, \lambda_0; q)/\cos k$, are presented in Figs. 1 and 2, which include the dependence on the parameters λ_0 and ζ , respectively.

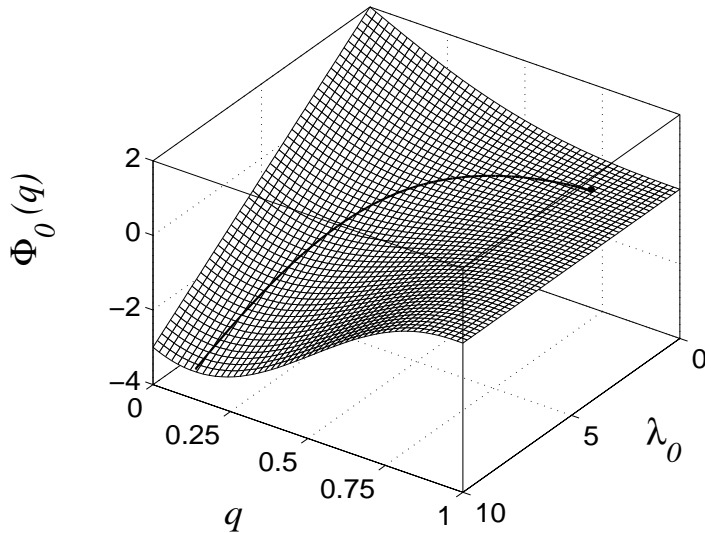


FIG. 1. Variational function $\Phi_0(q)$ plotted as a two-dimensional surface against q and λ_0 at the fixed value of the parameter b ($\zeta = 1.25$). The curve on this surface shows the set of minima of the function $\Phi_0(q, \lambda_0)$.

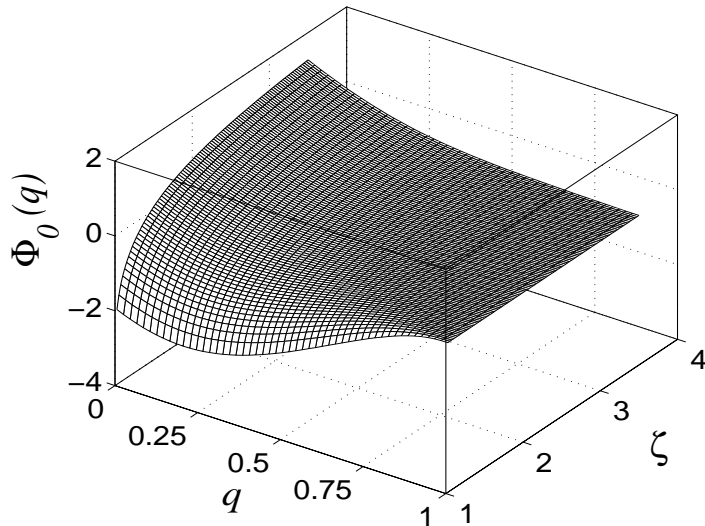


FIG. 2. Variational function $\Phi_0(q)$ plotted as a two-dimensional surface against q and ζ at the fixed value $\lambda_0 = 5$.

Both these plots show that the minimum of the variational energy $\Phi_0(q)$ disappears, for sufficiently small coupling constant λ_0 at ζ fixed (see Fig. 1 and the curve on the surface), or sufficiently large ζ at λ_0 fixed (see Fig. 2). This is contrary to the limiting case $\zeta \rightarrow 1$, when there exists the continuous transition from the small polaron regime to the large one if the constant λ_0 tends to zero. In other words, the polaron regime for a sufficiently big parameter b or a sufficiently weak coupling constant λ_0 , at certain critical values of these parameters, suddenly disappears.

Figure 3 shows details of the drastic behaviour of the energy function $\Phi_0(q)$. Here, curve 1 represents the energy behaviour of the system in the limiting case $\zeta = 1$, when the on-site potential is absent. In this case there exists only one minimum in the interval $0 < q < 1$ that corresponds to the polaron solution being a ground state of the system. After we introduce an on-site potential ($\zeta > 1$), the energy surface changes, and another local minimum appears at $q = 1$ (see curve 2 in the inset of Fig. 3).

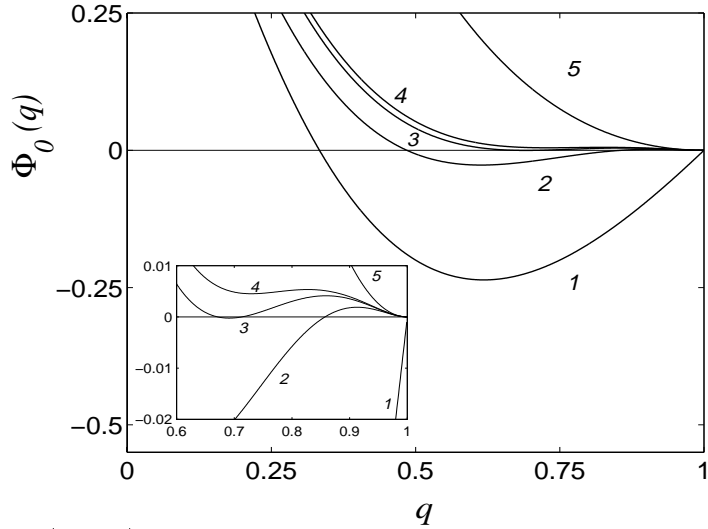


FIG. 3. Variational function $\Phi_0(\zeta, \lambda_0; q)$ against the parameter q for different values of the parameters ζ and λ_0 : $\zeta = 1$ and $\lambda_0 = 1$ (curve 1), $\zeta = 1.3$ and $\lambda_0 = 2$ (curve 2), $\zeta = 1.3875$ and $\lambda_0 = 2$ (curve 3), $\zeta = 1.415$ and $\lambda_0 = 2$ (curve 4), and $\zeta = 12.5$ and $\lambda_0 = 2$ (curve 5).

This minimum, at which the variational energy $\Phi_0(q)$ always equals zero (see (34)), corresponds to the extended, completely delocalized state. When we decrease λ_0 (at ζ fixed) or increase ζ (at λ_0 fixed), the size of the polaron profile increases and the energy minimum becomes more and more shallow. At a certain critical value of λ_0 or ζ , the variational energy at both the minima becomes the same (equal to zero) as demonstrated by curve 3 in Fig. 3. Further decrease of λ_0 or increase of ζ results in increasing the energy at the self-localized state which becomes positive, exceeding the zero energy of the delocalized state. Therefore the polaron state becomes metastable, whereas the delocalized state becomes a ground state. This situation is illustrated by curve 4 in Fig. 3. Finally, with further decreasing λ_0 or increasing ζ , the polaron state disappears and only one minimum at $q = 1$, which corresponds to the delocalized state, remains (see curve 5).

Thus, we have obtained three possible regimes: (i) the polaron is a ground state and the delocalized state is metastable, (ii) the polaron state is metastable and the delocalized state is a ground state, and (iii) the polaron does not exist and only the delocalized state is possible. A similar situation takes place in the other three cases described by the variational energies E_{S1} , E_{B0} , and E_{B1} .

Having found an optimal value of the variational parameter q for each set of the system parameters, one can plot a corresponding two-component polaron profile: the envelope φ_n (using (31) and (35)) and the displacement field u_n (using (32), (33), (36), and (37)). Figure 4 demonstrates the site-centred polaron profiles for the case $\eta = 0$ and two sets of the parameters which correspond to curves 2 and 3 in Fig. 3.

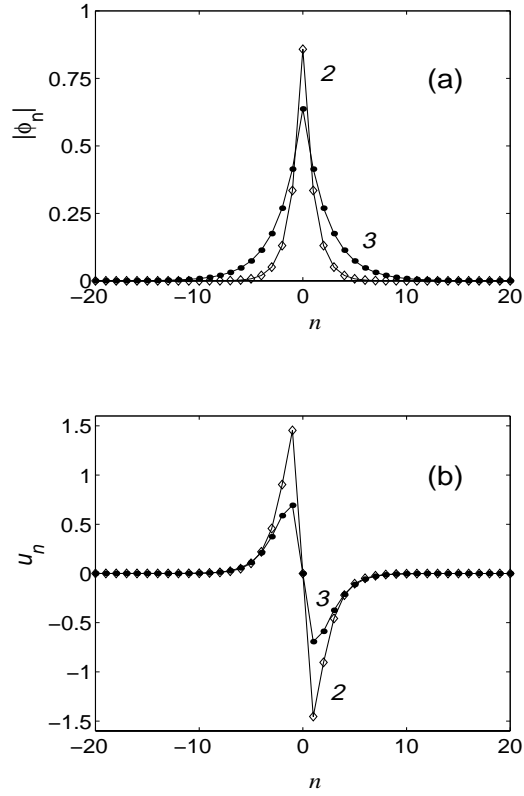


FIG. 4. Site-centred polaron profiles for $\eta = 0$: (a) wavefunction envelope φ_n , and (b) displacement field u_n correspond to the minima of the variational function $\Phi_0(q)$ plotted as curves 2 and 3 in Fig. 3. The system parameters for curves 1 and 2 are the same as for curves 2 and 3 in Fig. 3, respectively.

The bond-centred polaron profile for the case $\eta = 1$ is presented in Fig. 5.

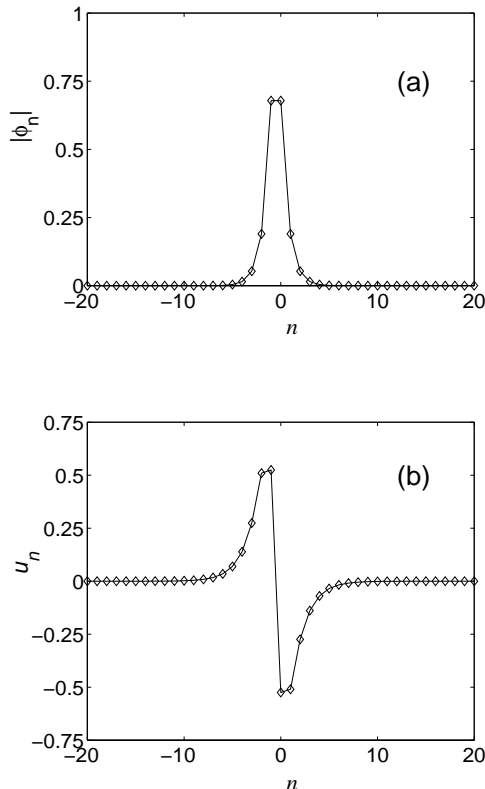


FIG. 5. Bond-centred polaron profiles for $\eta = 1$, $\zeta = 1.25$, and $\lambda_1 = 4$: (a) wavefunction envelope φ_n , and (b) displacement field u_n components.

V. A CRITERION FOR THE EXISTENCE OF SELF-LOCALIZED STATES

As demonstrated in the previous section, the variational functions $E_{S\nu}(b, \lambda_\nu; q)$ and $E_{B\nu}(b, \lambda_\nu; q)$, $\nu = 0, 1$, given by (34), (38), and (B1), do not always admit minima that correspond to self-localized states. To analyse them, it is convenient to represent the equations for extrema $\partial E_{S\nu}/\partial q = 0$ and $\partial E_{B\nu}/\partial q = 0$ in the form

$$F(b; q) \equiv \frac{1 - q^2}{(b - q^2)^3} W(b; q) = \frac{1}{\lambda} \quad (39)$$

where the subscripts $S\nu$ and $B\nu$ have been omitted for a while. The explicit form of the functions $W(b; q)$ is given in Appendix B (see (B2)) and the constants λ (with subscript ν also omitted) are defined by (A5) and (A10). Since each W is a weakly varying function which is bounded from above, it follows from (39) that for any $b > 1$, there exist sufficiently small values of the parameter λ when (39) does not possess a solution. On the other hand, in the case without any on-site potential ($b = 1$), the polaron solutions are known to exist for any constant $\lambda > 0$. Indeed, in the limit $b \rightarrow 1$, (39) becomes

$$\frac{q}{1 - q} = \frac{Y(q)}{\lambda}, \quad (40)$$

with the function $Y(q)$ given explicitly in Appendix B for each particular case (see (B3)). The left-hand side of Eq. (40) is a monotonically increasing function from zero to infinity and therefore for any λ this equation always admits a unique solution. This solution corresponds to the Davydov soliton in an isolated molecular chain [1–3,7,18].

The situation changes drastically in the case $b > 1$, when the left-hand side of Eq. (39) becomes a convex function which equals zero at $q = 0$ and $q = 1$. Let $q_m = q_m(b)$ be the point in the interval $0 < q < 1$ at which the function $F(b; q)$ attains a maximum. If the coupling constant λ is large enough, the line $1/\lambda$ will cross the curve $F(b; q)$ at two points, so that Eq. (39) will have two roots corresponding to extrema of the variational energy. The smaller root corresponds to a (polaron) minimum of the energy, while the bigger root corresponds to a maximum of this energy that separates the polaron minimum and the minimum at $q = 1$ responsible for the delocalized state.

With decreasing λ , these two extremal points move towards each other and eventually merge at some critical value of λ . With further decrease of λ , the polaron solution disappears completely. We denote $\mathcal{B}(b) \equiv \max_q F(b; q) = F[b; q_m(b)]$. Then the condition for the existence of polaron solutions, i.e., roots of (39), is the inequality

$$\mathcal{B}(b)\lambda > 1. \quad (41)$$

Therefore the (b, λ) -plane can be split into two regions by the line $\mathcal{B}(b)\lambda = 1$. This line separates the regions of existence and non-existence of self-localized states.

To be more precise, we consider first the site-centred solutions with $\eta = 0$ and fix the value $b = 2$. In this case, the function $F(2; q)$ has a maximum at the point $q_m = \sqrt{2/3}$. Inserting this value for q_m into the equation $F(2; q_m) = \lambda_0^{-1}$, we find the critical value of λ_0 at which the self-trapping appears. The self-trapped state exists for all $\lambda_0 > 4(2/3)^{5/2}$.

In the general case, with any $b > 1$, differentiating the function $F(b; q)$ with respect to q , equating the resulting expression to zero, and solving the resulting equation, we find the value q_m in the interval $0 < q < 1$ at which the function $F(b; q)$ reaches a maximum:

$$q_m^2 = \frac{5b^2 - 8b + 5 - (b-1)\sqrt{25b^2 - 22b + 25}}{2(2-b)}. \quad (42)$$

This expression is well defined for all $b > 1$, including the particular case $b = 2$ mentioned above, as well as the limit $b \rightarrow \infty$ for which $\lim_{b \rightarrow \infty} q_m^2 = 2/5$. In Fig. 6(a) we have plotted the line $\lambda_0 = \mathcal{B}_{S_0}^{-1}(b) = F[b; q_m(b)]^{-1}$ as a solid curve.

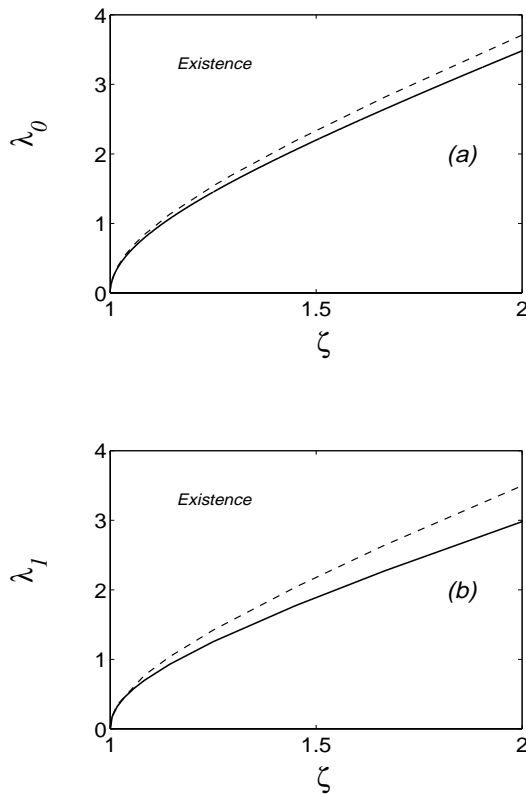


FIG. 6. Diagrams of existence of site-centred polaron states for (a) $\eta = 0$, and (b) $\eta = 1$. Solid curves separate the regions of existence and non-existence of polaron solutions, while dashed curves separate stable and metastable polaron solutions.

This curve separates the regions of existence and non-existence of polaron states. The dashed line, calculated by comparing the energy (34) in different polaron states with the zero energy (at $q = 1$), separates stable and metastable polaron states. Similar diagrams of the existence of site-centred self-localized solutions have been plotted in Fig. 6(b) for the case $\eta = 1$. In this case, there are no analytical solutions like (42) and therefore both the solid and dashed lines, with the same meaning as in Fig. 6(a), were calculated numerically, using (34), (39), and (41).

VI. BINDING ENERGY OF THE SELF-LOCALIZED (QUASI)PARTICLE

The dimensionless binding energy of the (quasi)particle ε , which can be calculated according to (12), is the lowest energy level of the Schrödinger equation (8). Using the envelope φ_n and the displacement field u_n given by (31)-(33) and (35)-(37) as well as the definitions (A5) and (A10), this energy can be expressed through the variational parameter q . The resulting equations are

$$\frac{\varepsilon}{\cos k} = 2 \frac{(1-q)^2}{1+q^2} - 2\lambda_\nu \frac{(1-q^2)^3}{(b-q^2)^2} P_{S\nu}(b; q), \quad \nu = 0, 1, \quad (43)$$

for the S self-trapped states and

$$\frac{\varepsilon}{\cos k} = (1-q)^2 - 2\lambda_\nu \frac{(1-q^2)^3}{(b-q^2)^2} P_{B\nu}(b; q), \quad \nu = 0, 1, \quad (44)$$

for the B self-trapped states.

In the particular case $\eta = 0$ and $k = 0$, the discrete Schrödinger equation (8) can be rewritten in the form

$$-(\varphi_{n+1} - 2\varphi_n + \varphi_{n-1}) + U_n \varphi_n = \varepsilon \varphi_n \quad (45)$$

where $U_n = \alpha(u_{n+1} - u_{n-1})/2$ is the deformation potential formed in the chain by a (quasi)particle (an excitation or an electron). The energy level ε and the potential U_n were calculated by minimization of the discrete energy functional (30), resulting in a numerically exact polaron solution, and then inserting this solution into (12). The results of these numerical calculations have confirmed the analytical results given by (32), (33), (36), (37), (43), and (44) to very high accuracy. Figure 7 illustrates, for the case $\eta = 0$, the comparison of the variational approximation given by the trial function (31) with the corresponding numerically exact polaron solution found by minimization of the energy (30).

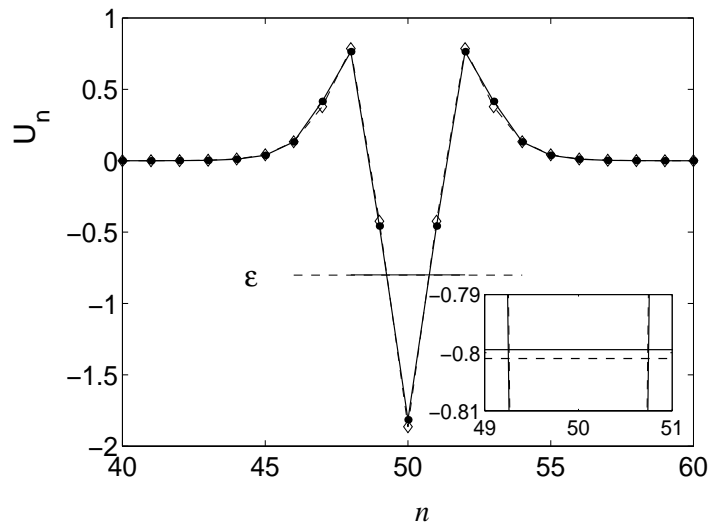


FIG. 7. Effective deformation potential U_n and the lowest energy level ε calculated numerically (solid lines) and analytically (dashed lines) for $\eta = 0$ ($\alpha = 4$, $\beta = 5$, $\lambda_0 = 5$, and $\zeta = 2$). The inset shows an enlargement of the η level curve.

VII. PINNING AND MOBILITY OF POLARONS

In general, while propagating along the chain, a narrow polaron (or another solitary wave, except for the supersonic pulse soliton in the Fermi-Pasta-Ulam type chain) radiates small-amplitude waves, and finally stops because of a so-called Peierls-Nabarro (PN) periodic potential relief. The existence of such a relief (barrier) is an effect of lattice discreteness [26]. In this section we extend the studies of the PN barrier for the Davydov soliton, carried out previously [27] for the case of an isolated molecular chain, to the case with an on-site potential ($b > 1$).

According to Eqs. (34) and (38), we have calculated the polaron energy in the S and B states for $\eta = 0$ and $\eta = 1$. Particularly, for the case $\eta = 0$ with $b = 1$ at $k = 0$ and for the same system parameters, the energy in the S state given by Eq. (34) appeared to be lower than that in the B state which is given by Eq. (38). This result coincides with

that found previously [27], i.e., the site-centred profile corresponds to a minimum of the polaron energy, whereas the bond-centred profile is associated with a saddle point. Surprisingly, similar calculations of the energies (34) and (38) for the case $\eta = 1$ gave the opposite energy inequality: the B self-localized state was found to have lower energy than the S state. Thus, for standing ($k = 0$) self-localized states the following two inequalities: $E_{S0} < E_{B0}$ and $E_{B1} < E_{S1}$ hold. Therefore one can expect that for a certain intermediate value $\eta = \eta_c$, the barrier defined by the difference $\Delta E = \Delta(\eta) \equiv |E_B(\eta) - E_S(\eta)|$ will disappear, so that the equality $\Delta E(\eta_c) = 0$ should be valid. For this purpose, we have calculated numerically the height of this barrier as a function of η , minimizing the energy functional (30). The dependencies $\Delta E = \Delta E(\eta)$ (solid line) and $E_B(\eta) - E_S(\eta)$ (dashed line) for $\lambda = 5$ (see (16), $k = 0$) and $\zeta = 2$ are shown in Fig. 8 that demonstrate the existence of a critical value η_c at which the $\Delta E = 0$ barrier entirely disappears.

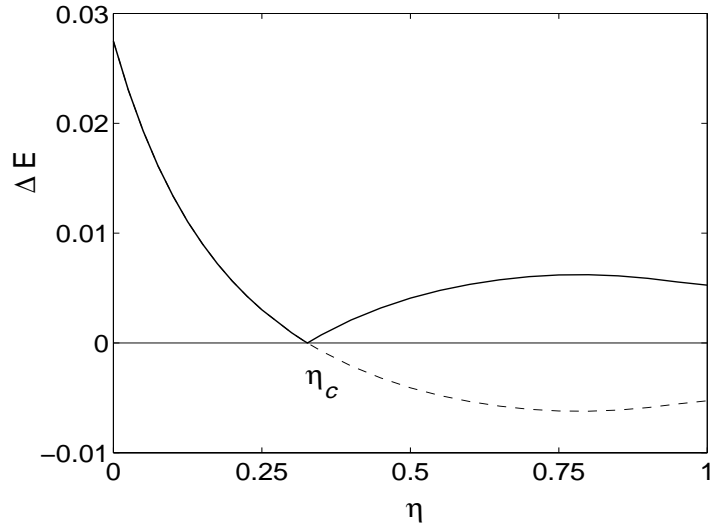


FIG. 8. Height of the pinning barrier ΔE (solid line) and the energy difference $E_B - E_S$ (dashed line) as functions of the parameter η for $\lambda = 5$ and $\zeta = 2$.

We have calculated this critical value for different system parameters. These results are presented in Table I.

TABLE I. Dependence of the critical value η_c on the strength of the on-site potential κ_0 and the coupling parameter λ .

λ	$\kappa_0 = 0.25$	$\kappa_0 = 0.5$	$\kappa_0 = 1$	$\kappa_0 = 2$	$\kappa_0 = 3$
2	0.3339	0.3316	-	-	-
5	0.3385	0.3357	0.3315	0.3266	0.3229
10	0.3429	0.3395	0.3355	0.3295	0.3260

They show that the critical value η_c depends very weakly on the system parameters and remains within the interval $0.32 \sim 0.35$. Increase of the coupling constant $\lambda = \alpha\beta/4$ or decrease of the on-site parameter κ_0 causes insignificant shift of η_c towards higher values. Note that ΔE is not a Peierls-Nabarro (PN) barrier, but just its estimate from below.

Such a behaviour of the pinning barrier gives us a reason to expect that a movable polaron can exist which does not experience any lattice effects. In order to check this, we simulated equations of motion (5) and (6) for the critical value $\eta_c = 0.325965$, using the fourth order Runge-Kutta scheme with the time step $\Delta\tau = 0.02$. This case should correspond to the transparent polaron motion through the chain, despite the fact that the parameter values were chosen to form a quite narrow polaron profile. Therefore we have substituted the polaron solution obtained before by minimization of the functional (30) into the basic equations of motion (5) and (6) reduced to the corresponding dimensionless form through the scaled wavefunction $\phi_n(\tau)$ and displacement field $u_n(\tau)$. The initial conditions were chosen according to the relations $du_n/d\tau \simeq -s(u_{n+1} - u_n)$ and $\phi_n(0) = \varphi_n \exp(ikn)$ where φ_n and u_n represent the polaron solution found by minimization of the energy (30). Here we have approximately replaced the time derivative by the spatial derivative. This is, of course, a very crude approximation for narrow polaron profiles, but it gives a proper initial kick to the polaron. We have chosen the wavevector $k = 0.4$ that corresponds to the velocity $s = 2\sigma \sin k \simeq 0.78$. The results of simulations are presented in Fig. 9.

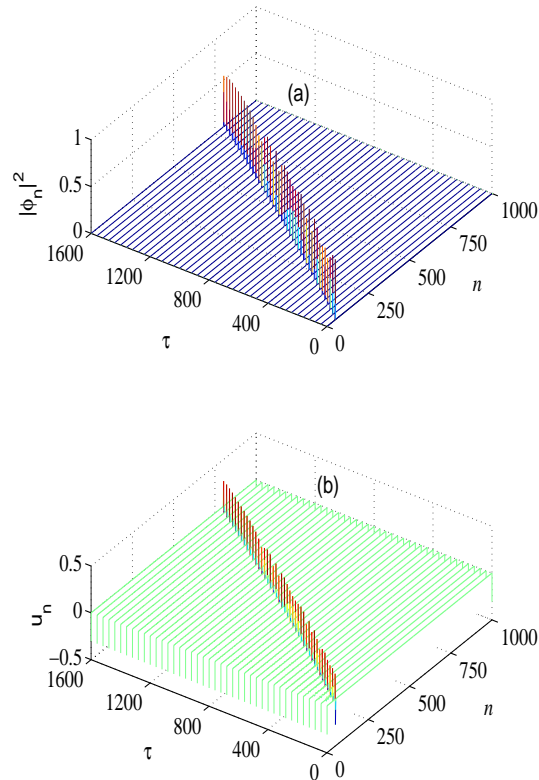


FIG. 9. Dynamics of lattice fields (a) $|\phi_n(\tau)|^2$, and (b) $u_n(\tau)$, in the chain consisting of $N = 1000$ particles ($\alpha = 10$, $\beta = 4$, $\zeta = 2.5$, $\sigma = 1$, and $\eta = \eta_c = 0.325965$).

Initially, right after the initial kick, the polaron emits some radiation and slows down, but later it separates itself from the radiation and propagates with constant velocity which is quite close to $s = 0.78$. The final snapshot of the polaron profile is presented in Fig. 10.

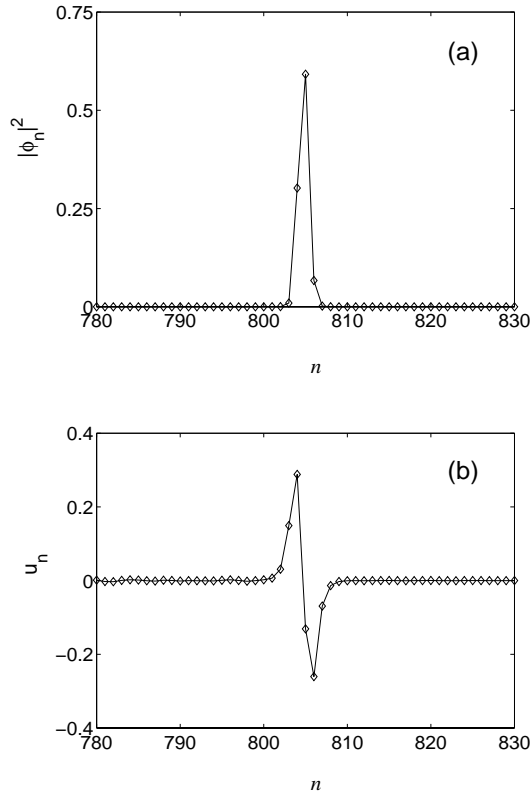


FIG. 10. Final polaron profiles of lattice fields (a) $|\phi_n(\tau_f)|^2$, and (b) $u_n(\tau_f)$, at final time instant $\tau = \tau_f = 1600$, the dynamics of which is displayed in Fig. 9.

As can be seen in these plots, the profile appears to be very narrow, propagating without significant energy loss. Some tiny radiation can be explained by very crude approximation of the initial conditions.

In order to emphasize the depinning effect, we performed similar simulations for η slightly different from the critical value. We took $\eta = 0.24$, while the rest of the system parameters were kept unchanged, and created the initial conditions in the same way as before. In this case, the polaron did not manage to move further than 12 chain sites and eventually got pinned. The results of these simulations are presented in Fig. 11.

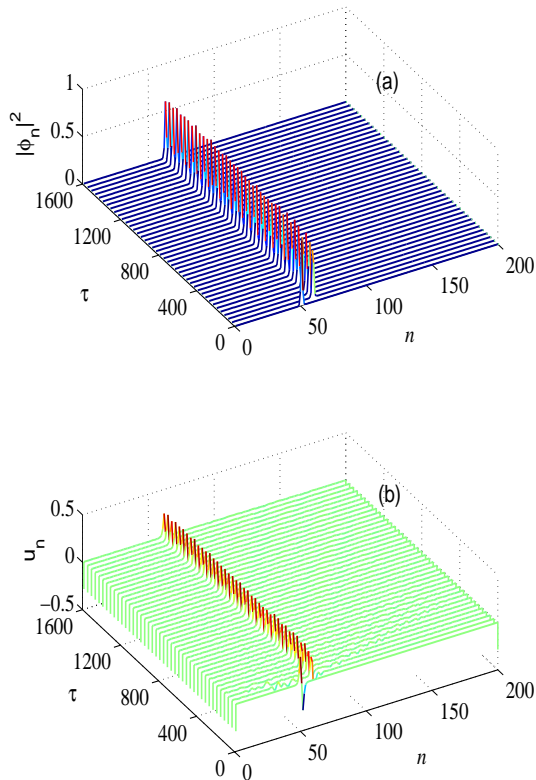


FIG. 11. Dynamics of lattice fields (a) $|\phi_n(\tau)|^2$ and (b) $u_n(\tau)$ in the chain with $N = 1000$ particles ($\alpha = 10$, $\beta = 4$, $\zeta = 2.5$, $\sigma = 1$, and $\eta = 0.24$).

VIII. CONCLUSIONS

Contrary to the one-dimensional acoustic polaron (Davydov-Scott) theory [1,2]), where the self-trapping occurs for all values of the system parameters, we have shown in this paper that the presence of a physically reasonable external on-site potential for each chain molecule leads in some cases to the non-existence of self-localized (polaron) states. It happens that for some parameter values the self-trapping exists, while for other values only delocalized states are possible. We have found the criterion for the existence of self-localized states given by the inequality (41). In particular, for the existence of polaron states the (quasi)particle-lattice coupling constant χ_1 or χ_2 should be sufficiently large or the strength κ_0 of the on-site potential should be sufficiently weak. This criterion is also valid for narrow polaron solutions which are immobile, so that even for standing one-dimensional polarons, their formation depends on the system parameters.

It is important to note that the delocalized (exciton) state does always exist in the chain, being therefore in some cases stable (a ground state) and in other cases metastable. More precisely, the following three regimes (three types of solutions) can exist in the chain with an on-site potential: (i) the polaron as a ground state and the exciton as a metastable state, (ii) the polaron as a metastable state and the exciton as a (delocalized) ground state, and (iii) the polaron state does not exist and only the exciton is a ground state. The analytical calculations performed in this paper allow us to investigate the physical mechanisms of the existence and non-existence of the self-trapping and to find two characteristic parameters b and λ , in terms of which we were able to formulate the criterion of the polaron existence (see (41)). In the simplest case when the polaron is standing and $\chi_2 = 0$, these parameters are $b = 1 + \kappa_0/2K + \sqrt{\kappa_0/K + (\kappa_0/2K)^2}$ and $\lambda = \chi^2 l^2 / JK$. For moving polarons the ratio κ_0/K and the reduced coupling constant λ are renormalized accordingly. If the on-site potential is sufficiently strong or the (quasi)particle-phonon coupling is sufficiently weak, the chain particles prefer to stay in the well of the on-site potential and the exciton-phonon interaction cannot displace them from the potential minima to support a stationary travelling-wave motion along the chain of a self-localized state. As illustrated by Fig. 3, the existence of both self-localized and delocalized solutions results in the appearance of an effective barrier that separates these states.

Although analytical calculations and techniques appear to be very lengthy and complicated, the final results presented by the variational functions (34) and (38) seem to be simple, and these are the main findings of the present

paper. We have introduced a whole variety of series which we call hyperbolic Chebyshev polynomials. This approach can be applied to other models of the polaron theory.

Surprisingly, it was found that stable self-localized states appear to occur with different (on-site or on-bond) symmetry. This is due to the different physical meaning of the coupling constants χ_1 and χ_2 mentioned in Introduction. This result prompted us to seek the ratio of these constants when depinning of a polaron occurs. We have found that it happens at the value $\eta = \chi_2/(\chi_1 + \chi_2) \simeq 0.33$ and confirmed by simulations that the polaron in the chain with this ratio can propagate freely, similarly to transparent propagation of narrow topological defects in discrete nonlinear Klein-Gordon systems [28].

ACKNOWLEDGMENTS

YZ wishes to acknowledge the financial support from Heriot-Watt University and the Max-Planck-Institut für Physik Komplexer Systeme. We are also grateful for support under the LOCNET EU network HPRN-CT-1999-00163. Useful discussions with S. Aubry are also acknowledged.

APPENDIX A: DISPLACEMENT FIELDS AND CORRESPONDING DNLS EQUATIONS

1. Site-centred self-localized states

a. The case $\eta = 0$ ($\chi_1 > 0$, $\chi_2 = 0$)

Using (15) for the particular case $\eta = 0$, the result (25) can be rewritten in terms of φ_j^2 , $j = 0, 1, \dots$, as follows

$$u_1 = G \left[- (b^{-1}\varphi_0^2 + b^{-2}\varphi_1^2) + (b - b^{-1}) \sum_{j=2}^{\infty} b^{-j}\varphi_j^2 \right]. \quad (\text{A1})$$

In this series, the first two terms are negative while the others are positive. Substituting the series (A1) into (19) where R_j is defined by (15) with $\eta = 0$ and using the representation for the polynomials $K_n^{[2\zeta]}$ given by (24), we find the following series for the displacement u_n :

$$u_n = G \sum_{j=0}^{\infty} A_{jn}\varphi_j^2, \quad n \geq 1, \quad (\text{A2})$$

where the matrix coefficients A_{jn} , $j = 0, 1, \dots$, $n = 1, 2, \dots$, are given by

$$\begin{aligned} A_{0n} &= -b^{-n}, \quad n \geq 1; \\ A_{jn} &= - (b^j + b^{-j}) b^{-n}, \quad 1 \leq j \leq n-1, \quad n \geq 2; \\ A_{nn} &= -b^{-2n}, \quad n \geq 1; \\ A_{jn} &= b^{-j} (b^n - b^{-n}), \quad j \geq n+1, \quad n \geq 1. \end{aligned} \quad (\text{A3})$$

Using the series representation (A2) in (8) with $\eta = 0$, we get the following stationary discrete nonlinear Schrödinger (DNLS) equation:

$$\varphi_{n+1} - 2\varphi_n + \varphi_{n-1} + \lambda_0 \sum_{j=0}^{\infty} (A_{j,n-1} - A_{j,n+1}) \varphi_j^2 \varphi_n + (\varepsilon/\cos k)\varphi_n = 0, \quad n \geq 0, \quad (\text{A4})$$

where $A_{j0} = 0$, $A_{j,-1} = A_{j1}$, and $\varphi_{-1} = \varphi_1$. Here the (quasi)particle-phonon coupling parameter λ_0 is given through the expression for λ defined by (16):

$$\lambda_0 \equiv \lambda|_{\eta=0} = \alpha\beta/4(1 - s^2)\cos k. \quad (\text{A5})$$

b. *The case $\eta = 1$ ($\chi_1 = 0, \chi_2 > 0$)*

Similarly, using the expression (15) at $\eta = 1$, the series (25) is rewritten in terms of $\varphi_j \varphi_{j+1}$, $j = 0, 1, \dots$, as follows

$$u_1 = 2G \cos k \left[-b^{-1} \varphi_0 \varphi_1 + (1 - b^{-1}) \sum_{j=1}^{\infty} b^{-j} \varphi_j \varphi_{j+1} \right]. \quad (\text{A6})$$

Here the first term is negative while the others are positive. In the same way as above, using Eq. (15) with $\eta = 1$, the explicit formula (24), and the series (A6), we find that the series (19) is transformed to

$$u_n = 2G \cos k \sum_{j=0}^{\infty} B_{jn} \varphi_j \varphi_{j+1}, \quad n \geq 1, \quad (\text{A7})$$

where the coefficients B_{jn} , $j = 0, 1, \dots$, $n = 1, 2, \dots$, are given by

$$\begin{aligned} B_{0n} &= -b^{-n}, \quad n \geq 1; \\ B_{jn} &= -\frac{1}{b+1} (b^{j+1} + b^{-j}) b^{-n}, \quad 1 \leq j \leq n-1, \quad n \geq 2; \\ B_{jn} &= \frac{1}{b+1} b^{-j} (b^n - b^{-n}), \quad j \geq n \geq 1. \end{aligned} \quad (\text{A8})$$

In the similar way, using the series (A7), equation (8) at $\eta = 1$ is transformed to

$$\varphi_{n+1} - 2\varphi_n + \varphi_{n-1} + 2\lambda_1 \sum_{j=0}^{\infty} [(B_{j,n-1} - B_{jn}) \varphi_{n-1} + (B_{jn} - B_{j,n+1}) \varphi_{n+1}] \varphi_j \varphi_{j+1} + (\varepsilon/\cos k) \varphi_n = 0, \quad n \geq 0, \quad (\text{A9})$$

where $B_{j0} = 0$, $B_{j,-1} = -B_{j1}$, and $\varphi_{-1} = \varphi_1$. The reduced coupling parameter λ_1 is given by (see (16))

$$\lambda_1 \equiv \lambda|_{\eta=1} = \alpha\beta \cos k / 4(1 - s^2). \quad (\text{A10})$$

2. Bond-centred self-localized states

The case $\eta = 0$ ($\chi_1 > 0, \chi_2 = 0$). In the same way as for the S states, using Eq. (15) for the particular case $\eta = 0$, the series (29) can be rewritten in terms of φ_j^2 , $j = 1, 2, \dots$, as follows

$$u_1 = G \left[-b^{-1} \varphi_1^2 + (b-1) \sum_{j=2}^{\infty} b^{-j} \varphi_j^2 \right] \quad (\text{A11})$$

where we have used the relation $\varphi_0 = \varphi_1$ (see (18)). The first term of the series (A11) is negative while the others are positive. Substituting next the series (A11) into Eq. (26) where R_j is defined by Eq. (15) with $\eta = 0$ and using the representation for the polynomials $K_n^{[2\zeta]}$ and $K_n^{[2\zeta+1]}$ given by Eqs. (24) and (28), we find the displacement field u_n in the as a series

$$u_n = G \sum_{j=1}^{\infty} C_{jn} \varphi_j^2, \quad n \geq 1, \quad (\text{A12})$$

where the matrix coefficients C_{jn} , $j, n = 1, 2, \dots$, are given by

$$\begin{aligned} C_{nn} &= -b^{-2n+1}, \quad n \geq 1; \\ C_{jn} &= -(b^j + b^{-j+1}) b^{-n}, \quad 1 \leq j \leq n-1, \quad n \geq 2; \\ C_{jn} &= b^{-j} (b^n - b^{-n+1}), \quad j \geq n+1, \quad n \geq 1. \end{aligned} \quad (\text{A13})$$

Similarly, using the series representation (A12) in (8) with $\eta = 0$, one obtains the stationary DNLS equation

$$\varphi_{n+1} - 2\varphi_n + \varphi_{n-1} + \lambda_0 \sum_{j=1}^{\infty} (C_{j,n-1} - C_{j,n+1}) \varphi_j^2 \varphi_n + (\varepsilon/\cos k) \varphi_n = 0, \quad n \geq 1, \quad (\text{A14})$$

where $C_{j0} = -C_{j1}$, $\varphi_0 = \varphi_1$, and the coupling constant λ_0 is given by Eq. (A5).

a. The case $\eta = 1$ ($\chi_1 = 0, \chi_2 > 0$)

In the same way as for the S states, using the expression (15) at $\eta = 1$, the series (29) is rewritten in terms of $\varphi_j \varphi_{j+1}$, $j = 0, 1, \dots$, as

$$u_1 = \frac{2G \cos k}{b+1} \left[-\varphi_1^2 + (b-1) \sum_{j=1}^{\infty} b^{-j} \varphi_j \varphi_{j+1} \right]. \quad (\text{A15})$$

As above, the first term in this series is negative while the others are positive. Using next (15) with $\eta = 1$, and inserting the expressions (24), (28), and (A15) into the series (26), we find

$$u_n = 2G \cos k \sum_{j=0}^{\infty} D_{jn} \varphi_j \varphi_{j+1}, \quad n \geq 1, \quad (\text{A16})$$

where $\varphi_0 = \varphi_1$ and the coefficients D_{jn} , $j = 0, 1, \dots$, $n = 1, 2, \dots$, are given by

$$\begin{aligned} D_{0n} &= -\frac{b^{-n+1}}{b+1}, \quad n \geq 1; \\ D_{jn} &= -\frac{1}{b+1} (b^j + b^{-j}) b^{-n+1}, \quad 1 \leq j \leq n-1, \quad n \geq 2; \\ D_{jn} &= \frac{1}{b+1} b^{-j} (b^n - b^{-n+1}), \quad j \geq n, \quad n \geq 1. \end{aligned} \quad (\text{A17})$$

Similarly, the corresponding DNLS equation is found from (8) with $\eta = 1$, using the representation (A16):

$$\varphi_{n+1} - 2\varphi_n + \varphi_{n-1} + 2\lambda_1 \sum_{j=0}^{\infty} [(D_{j,n-1} - D_{jn}) \varphi_{n-1} + (D_{jn} - D_{j,n+1}) \varphi_{n+1}] \varphi_j \varphi_{j+1} + (\varepsilon/\cos k) \varphi_n = 0, \quad n \geq 1, \quad (\text{A18})$$

where $D_{j0} = -D_{j1}$, $\varphi_0 = \varphi_1$, and the coupling constant λ_1 is given by (A10).

The nonlinearity in each of the stationary DNLS equations (A4), (A9), (A14), or (A18) contains infinite series which in the continuum limit are transformed to integral terms. It can easily be checked that in the limiting case $b \rightarrow 1$ the coefficients (A3), (A8), (A13), and (A17) take a simple form, so that the series in the corresponding DNLS equations are reduced to single cubic nonlinear terms.

APPENDIX B: THE P , W , AND Y FUNCTIONS AND THEIR BEHAVIOUR

The four functions $P(b; q)$ that appear in (34) and (38) are given by

$$\begin{aligned} P_{S0} &= \frac{b}{1+q^2}, \quad P_{S1} = \frac{4bq^2}{(1+q^2)^3}, \quad P_{B0} = \frac{1}{4} (2b+1-q^2), \\ P_{B1} &= \frac{(1-q) [(2b+q)q(1+q^2) + b(b+q^2)] + 2bq^2(b+q)}{(b+1)(1+q)(1+q^2)}. \end{aligned} \quad (\text{B1})$$

The functions (B1) have small variation in the interval $0 \leq q \leq 1$ and each of them tends to $b/2$ if $q \rightarrow 1$.

The other four functions $W(b; q)$ which are involved in (39) as factors have also small variation and are given explicitly by

$$\begin{aligned} W_{S0} &= bq(2b-1+bq^2-2q^2), \\ W_{S1} &= \frac{2bq}{(1+q^2)^2} (-b+6bq^2-q^2+bq^4-6q^4+q^6), \\ W_{B0} &= \frac{1}{2} q(1+q)(3b^2-1-3bq^2+q^4), \\ W_{B1} &= \frac{1}{(b+1)(1+q^2)^2} \{ (b-1) [b^2(1+q-q^2+8q^3-q^4+5q^5) \\ &\quad + bq(1+q+6q^2+14q^3-9q^4+7q^5-8q^6) \\ &\quad + q^3(7+6q-3q^2-8q^3-6q^5+3q^6)] + 2q^3(1-q^2)(1+q)(3-q^4) \}. \end{aligned} \quad (\text{B2})$$

In each of the four cases $S\nu$ and $B\nu$, $\nu = 1, 2$, the functions $Y(q)$ [see Eq. (40)] are defined by

$$\begin{aligned} Y_{S0} &= 1 + q, & Y_{S1} &= \frac{(1+q)(1+q^2)^2}{2(4q^2-1-q^4)}, \\ Y_{B0} &= \frac{2}{2-q^2}, & Y_{B1} &= \frac{(1+q^2)^2}{q^2(3-q^4)}. \end{aligned} \tag{B3}$$

All these four functions have the same limit ($Y \rightarrow 2$) when $q \rightarrow 1$.

- [1] A. S. Davydov, *Solitons in Molecular Systems* (Reidel, Dordrecht, 1991).
- [2] A. C. Scott, Phys. Rep. **217**, 1 (1992).
- [3] L. Cruzeiro-Hansson and S. Takeno, Phys. Rev. E **56**, 894 (1997).
- [4] Y. Zhao, D. W. Brown, and K. Lindenberg, J. Chem. Phys. **106**, 2728 (1997); **106**, 5622 (1997); **107**, 3159 (1997); D. W. Brown, K. Lindenberg, and Y. Zhao, *ibid.* **107**, 3179 (1997).
- [5] P. E. Kornilovitch and E. R. Pike, Phys. Rev. B **55**, 8634 (1997); P. E. Kornilovitch, Phys. Rev. Lett. **81**, 5382 (1998); A. S. Alexandrov and P. E. Kornilovitch, *ibid.* **82**, 807 (1999); P. E. Kornilovitch, Phys. Rev. B **59**, 13 531 (1999).
- [6] R. Roncaglia and G. P. Tsironis, Physica D **113**, 318 (1998).
- [7] A. M. Clogston, H. K. McDowell, P. Tsai, and J. Hanssen, Phys. Rev. E **58**, 6407 (1998).
- [8] Y. Zolotaryuk and J. C. Eilbeck, J. Phys.: Condens. Matter **10**, 4553 (1998).
- [9] E. Jeckelmann and S. R. White, Phys. Rev. B **57**, 6376 (1998); C. Zhang, E. Jeckelmann, and S. R. White, *ibid.* **60**, 14 092 (1999).
- [10] A. H. Romero, D. W. Brown, and K. Lindenberg, J. Chem. Phys. **109**, 6540 (1998); Phys. Lett. A **254**, 287 (1999); Phys. Rev. B **59**, 13 728 (1999).
- [11] G. Kalosakas, S. Aubry, and G. P. Tsironis, Phys. Rev. B **58**, 3094 (1998); Phys. Lett. A **247**, 413 (1998).
- [12] L. Proville and S. Aubry, Physica D **113**, 307 (1998); Eur. Phys. J. B **11**, 41 (1999).
- [13] D. Bambusi, J. Math. Phys. **40**, 3710 (1999).
- [14] S. Raghavan, A. R. Bishop, and V. M. Kenkre, Phys. Rev. B **59**, 9929 (1999).
- [15] L. Cruzeiro-Hansson, J. C. Eilbeck, J. L. Marín, and F. M. Russell, Phys. Lett. A **266**, 160 (2000).
- [16] A. S. Davydov and N. I. Kislukha, Phys. Status Solidi B **59**, 465 (1973).
- [17] S. Takeno, Prog. Theor. Phys. **71**, 395 (1984); **75**, 1 (1986).
- [18] A. C. Scott, Phys. Rev. A **26**, 578 (1982).
- [19] T. Holstein, Ann. Phys. (N.Y.) **8**, 325 (1959); **8**, 343 (1959).
- [20] G. Careri, U. Buontempo, F. Carta, E. Gratton, and A. C. Scott, Phys. Rev. Lett. **51**, 304 (1983); G. Careri, U. Buontempo, F. Galluzzi, A. C. Scott, E. Gratton, and E. Shyamsunder, Phys. Rev. B **30**, 4689 (1984).
- [21] J. C. Eilbeck, P. S. Lomdahl, and A. C. Scott, Phys. Rev. B **30**, 4703 (1984); Physica D **16**, 318 (1985).
- [22] A. V. Zolotaryuk, St. Pnevmatikos, and A. V. Savin, in *Davydov's Soliton Revisited*, edited by P. L. Christiansen and A. C. Scott (Plenum, New York, 1990), pp. 181-194; V. N. Kadantsev, L. N. Lupichov, and A. V. Savin (preprint).
- [23] Y. Zolotaryuk, Doctoral thesis, Heriot-Watt University, Edinburgh, 1998.
- [24] A. V. Zolotaryuk, K. H. Spatschek, and O. Kluth, Phys. Rev. B **47**, 7827 (1993).
- [25] W. C. Kerr and P. S. Lomdahl, Phys. Rev. B **35**, 3629 (1987).
- [26] M. Peyrard and M. D. Kruskal, Physica D **14**, 88 (1984).
- [27] V. A. Kuprievich, Physica D **14**, 395 (1985); A. A. Vakhnenko and Yu. B. Gaididei, Teor. Mat. Fiz. **68**, 350 (1986) [Sov. Theor. Math. Phys. **68**, 873 (1987)].
- [28] A. V. Savin, Y. Zolotaryuk, and J. C. Eilbeck, Physica D **138**, 267 (2000).